THE JOURNAL OF BIOLOGICAL CHEMISTRY VOL. 282, NO. 33, pp. 24198–24208, August 17, 2007

Asymmetric and Redox-specific Binding of Quinone and Quinol at Center N of the Dimeric Yeast Cytochrome bc_1 Complex

CONSEQUENCES FOR SEMIQUINONE STABILIZATION[*][S]

Received for publication, January 23, 2007, and in revised form, June 20, 2007 Published, JBC Papers in Press, June 21, 2007, DOI 10.1074/jbc.M700662200

Raul Covian[‡], **Klaus Zwicker**[§], **Frederik A. Rotsaert**[‡], **and Bernard L. Trumpower**[‡1]

From the [‡]*Department of Biochemistry, Dartmouth Medical School, Hanover, New Hampshire 03755 and the* [§]*Zentrum der Biologischen Chemie, Molekulare Bioenergetik, Universität Frankfurt, D-60590 Frankfurt am Main, Germany*

The cytochrome bc_1 complex recycles one of the two electrons from quinol (QH_2) oxidation at center P by reducing quinone (Q) at center N to semiquinone (SQ), which is bound tightly. We have analyzed the properties of SQ bound at center N of the yeast bc_1 complex. The EPR-detectable signal, which reports SQ bound in the vicinity of reduced b_H heme, was abolished by the center N inhibitors antimycin, funiculosin, and ilicicolin H, but was unchanged by the center P inhibitors myxothiazol and stigmatellin. After correcting for the EPR-silent SQ bound close to oxidized b_H, we calculated a midpoint redox potential (E_m) of ~90 mV for all bound SQ. Considering the E_m values for b_H and free Q, this result indicates that center N preferentially stabilizes SQ·b_H^{3+} complexes. This favors recycling of the electron coming from center P and also implies a >2.5-fold higher affinity for QH_2 than for Q at center N, which would potentially inhibit b_H oxidation by Q. Using pre-steady-state kinetics, we show that Q does not inhibit the initial rate of b_H reduction by QH_2 through center N, but does decrease the extent of reduction, indicating that Q binds only when b_H is reduced, whereas QH_2 binds when b_H is oxidized. Kinetic modeling of these results suggests that formation of SQ at one center N in the dimer allows stabilization of SQ in the other monomer by Q reduction after intradimer electron transfer. This model allows maximum SQ·b_H^{3+} formation without inhibition of Q binding by QH_2.

The cytochrome bc_1 complex couples electron transfer from QH_2 [2] to cytochrome *c* to a net movement of protons across the membrane in which it is embedded. This is achieved by having two QH_2/Q-binding sites (center P and center N) in cytochrome *b* close to opposite sides of the membrane, as is clearly seen in crystallographic structures (1–4). The bifurcated mechanism of QH_2 oxidation at center P in the protonmotive Q cycle results in one of the electrons from the substrate being transferred to the b_L heme and then to the b_H heme, which is in close proximity to the center N-binding pocket. This electron is used to reduce Q, producing an SQ intermediate, which is further reduced to QH_2 after a second oxidation event at center P. For proton translocation to occur, these two sites must function in opposite directions, so protons from QH_2 oxidation at center P are released to the positive side of the membrane, whereas Q reduction at center N results in proton uptake from the negative side.

However, the b_H heme group responsible for Q reduction at center N has a midpoint redox potential at pH 7 (E_{m7}) of 50–100 mV (5–7), which is close to the value of 60–90 mV for the Q pool in the membrane (8, 9). This implies that the b_H heme should oxidize QH_2 as easily as it can reduce Q. When electrons are prevented from flowing out of cytochrome *b* through center N, QH_2 oxidation at center P is inhibited and results in detrimental side reactions, such as superoxide formation (10, 11). We have recently provided evidence indicating fast electron equilibration between b_H hemes in the bc_1 complex dimer and suggested that this minimizes formation of inhibitory SQ·b_H^{2+} complexes at center N (12). Furthermore, potentiometric studies of SQ bound at center N (13–15) have indicated that the E_m of this intermediate is more positive than that of the Q pool by at least 20 mV, suggesting that formation of productive SQ·b_H^{3+} complexes is favored by preferential binding of QH_2 to center N. Nevertheless, this introduces another difficulty for optimal center N function because QH_2 would prevent binding of Q to center N, especially at high QH_2/Q ratios.

We have analyzed the thermodynamic properties of bound SQ and the pre-steady-state kinetics of b_H reduction through center N of the yeast bc_1 complex. Our results point to a mechanism in which center N sites in the dimer selectively bind QH_2 or Q depending on the redox state of the b_H heme as well as on the occupancy of the other monomer. We discuss how this model maximizes SQ·b_H^{3+} complex formation while preventing QH_2 from interfering with Q binding.

EXPERIMENTAL PROCEDURES

Materials—Dodecyl maltoside was obtained from Anatrace. Antimycin, myxothiazol, DBQ, and redox mediators were pur-

* This work was supported by National Institutes of Health Research Grant GM 20379. The costs of publication of this article were defrayed in part by the payment of page charges. This article must therefore be hereby marked "*advertisement*" in accordance with 18 U.S.C. Section 1734 solely to indicate this fact.

[S] The on-line version of this article (available at http://www.jbc.org) contains supplemental Fig. S1 and the complete DynaFit script files.

[1] To whom correspondence should be addressed: Dept. of Biochemistry, Dartmouth Medical School, 7200 Vail, Hanover, NH 03755. Tel.: 603-650-1621; Fax: 603-650-1128; E-mail: Trumpower@Dartmouth.edu.

[2] The abbreviations used are: QH_2, quinol; Q, quinone; SQ, semiquinone; DBQ, decylubiquinone; DBH_2, decylubiquinol (2,3-dimethoxy-5-methyl-6-decyl-1,4-benzoquinol); mT, milliteslas.

chased from Sigma, except for menaquinone, which was synthesized in the laboratory. Funiculosin was a gift from Novartis (Basel, Switzerland), and ilicicolin H was from the Merck sample repository. DBH_2 was prepared as described previously (16). All inhibitors and DBH_2 were quantified by UV spectroscopy (17) using previously reported extinction coefficients (18–20).

Purification of Cytochrome bc_1 Complex—Wild-type cytochrome bc_1 complex was isolated from Red Star cake yeast as described previously (21). Quantification of the bc_1 complex was performed as reported previously (22) using extinction coefficients of 17.5 mM^{-1} cm^{-1} at 553–539 nm for cytochrome c_1 (23) and 25.6 mM^{-1} cm^{-1} at 562–579 nm for the average absorbance of the b_H and b_L hemes in cytochrome *b* (24). The amount of endogenous Q copurified with the bc_1 complex was determined as described previously (12) and varied between different preparations in the range of 0.8–1.2 molecules/bc_1 monomer.

Semiquinone Redox Titration—Purified bc_1 complex was diluted with 100 mM Tris and 50 mM KCl (pH 7.4) to a final concentration of 24–30 μM (based on Rieske iron-sulfur cluster concentration as measured by EPR spectroscopy; see below). Upon addition of 33 μM 2,3,5,6-tetramethyl-*p*-phenylenediamine (E_{m7} = +270 mV) and 33 μM phenazine ethosulfate (E_{m7} = +55 mV) as redox mediators, the solution was transferred into an anaerobic vessel continuously flushed with argon. The appearance of additional artificial radical signals was avoided by using only two mediator dyes, one having its E_m in the range of the expected value of the Rieske iron-sulfur cluster and the other in the range of the expected E_m of SQ.

The sample was stirred at a constant temperature of 298 K and poised at desired potential values by adding small aliquots of 50 mM sodium dithionite solution. The potential was monitored by a redox microelectrode (Mettler-Toledo GmbH, Gieβen, Germany), and at appropriate values, 100 μl of the solution were transferred into argon-flushed EPR tubes (4-mm diameter), frozen in a cold isopentane/methyl cyclohexane mixture (5:1, ~120 K), and stored in liquid nitrogen until EPR measurements were taken. Usually, titrations started at potentials of +350 mV and were followed down to −120 mV. X-band EPR spectra were obtained with a Bruker ESP 300E spectrometer equipped with a Hewlett Packard HP 53159A frequency counter, a Bruker ER 035M NMR gaussmeter, and an Oxford Instruments liquid helium continuous flow cryostat. The degree of reduction of the Rieske iron-sulfur cluster was followed by recording EPR spectra at 20 K (microwave frequency, 9.47 GHz; microwave power, 2 milliwatts; modulation amplitude, 0.64 milliteslas (mT); and sweep width, 100 mT).

The appearance of SQ signals was detected at 50 K (microwave frequency, 9.47 GHz; microwave power, 0.01 milliwatt; modulation amplitude, 0.2 mT; and sweep width, 5 mT). A Q-free bc_1 preparation (25) was titrated in the same manner as the other samples to analyze the occurrence of any artificial radical signals or base-line drifts derived from mediator dyes or any other component in the solution. Although showing normal titration behavior of the Rieske iron-sulfur cluster, no EPR signal in the range of SQ radicals was detectable in this sample. For data analysis, all signal intensities of SQ radicals were normalized to the maximum intensity of the signal in the control titration, in the absence of any inhibitor. Quantitation of maximum SQ concentrations was achieved by accumulation of spectra at 50 K, subtraction of the spectrum of the Q-free sample, double integration, and comparison with spectra from galvinoxyl-free radical (Sigma) at known concentrations. For power saturation measurements, the modulation amplitude was decreased to 0.1 mT to avoid signal broadening, and the sweep time was doubled from 42 to 84 s. Saturation curves were fitted to a standard equation describing the behavior of one paramagnetic species (26).

Cytochrome b Redox Titration—Optical potentiometric titrations were performed at 24 °C in a 3.5-ml quartz cuvette as described previously (27). The potential was measured with a platinum-Ag/AgCl (3M) microelectrode (MI-80414-6, Microelectrodes, Inc.). All values are expressed with respect to the normal hydrogen electrode. The electrode was calibrated against a pH 7 standard solution of quinhydrone (E_m = +296 mV). The purified bc_1 complex was diluted to 2 μM in 100 mM Tris (pH 7.4), 50 mM KCl, and 0.01% dodecyl maltoside. Redox equilibration between the protein and the electrode was achieved by a mixture of the following dyes (with their E_{m7} values): 70 μM 2,3,5,6-tetramethyl-*p*-phenylenediamine (+270 mV), 25 μM 1,2-naphthoquinone (+144 mV), 25 μM phenazine methosulfate (+80 mV), 25 μM phenazine ethosulfate (+55 mV), 50 μM duroquinone (+5 mV), 30 μM menaquinone (−76 mV), 50 μM 2-hydroxy-1,4-naphthoquinone (−145 mV), 30 μM anthraquinone 2,6-disulfonate (−184 mV), and 30 μM anthraquinone 2-sulfonate (−225 mV).

A 10 or 100 mM solution of dithionite and ferricyanide was used for the reductive and oxidative titrations, respectively. The UV-visible spectra were recorded between 500 and 600 nm in an Aminco DW-2 dual-wavelength spectrophotometer in the split beam mode. The absorbance at 562 minus 578 nm was plotted against the potential (E_h) of the system. The reductive and oxidative titrations were averaged, and the resulting graph was fitted in the ORIGIN 5.0 program (OriginLab Corp.) to the following $n = 1$ Nernst equation (Equation 1) with two components to obtain the redox potential for the b_H ($E_{m(b_H)}$) and b_L ($E_{m(b_L)}$) hemes as well as the relative contribution of the b_H heme to the total absorbance (*b*),

$$\Delta A(562\text{–}578\ \text{nm}) = C\epsilon p\left(b\,\frac{e^{\frac{nF}{RT}(E_{m(b_H)} - E_h)}}{1 + e^{\frac{nF}{RT}(E_{m(b_H)} - E_h)}} + (1 - b)\,\frac{e^{\frac{nF}{RT}(E_{m(b_L)} - E_h)}}{1 + e^{\frac{nF}{RT}(E_{m(b_L)} - E_h)}}\right) \quad \text{(Eq. 1)}$$

where *C* is the concentration of bc_1 complex monomers (in this case, 2 μM), ϵ is the added extinction coefficient of both *b* hemes (51.2 mM^{-1} cm^{-1}), and *p* is the light path length (in this case, 1 cm). The temperature of the assay was maintained at 24 °C. The Nernst plots for both oxidative and reductive titrations were essentially identical, indicating full reversibility in the titration and confirming that the system was in equilibrium.

Pre-steady-state Reduction of Cytochrome b through Center N—Pre-steady-state reduction of cytochrome *b* was followed at 24 °C by stopped-flow rapid scanning spectroscopy using the

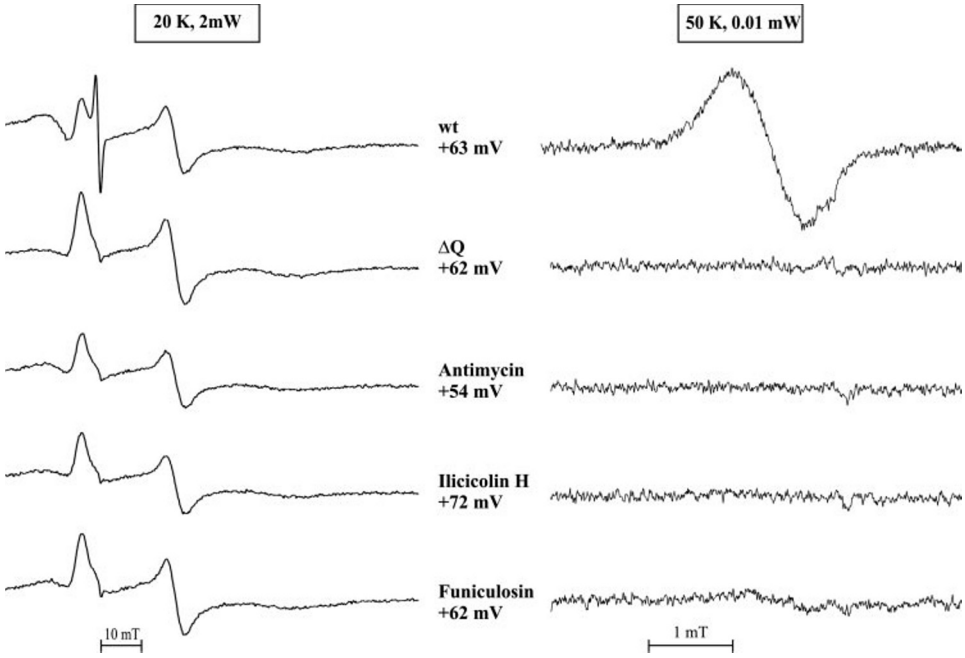

FIGURE 1. **EPR spectra of SQ at center N of the yeast bc_1 complex.** Data were collected at the indicated temperatures and microwave powers to reveal the EPR signature of the reduced Rieske protein together with the SQ signal (*left*) or to observe only the signal from SQ (*right*). The redox potential (E_h) of the system was poised approximately at the value that yielded the maximum SQ signal in the wild-type (*wt*) enzyme. When the bc_1 complex from a yeast strain lacking Q (Δ*Q*) was used or when antimycin, funiculosin, or ilicicolin H (~1.5 eq/monomer) was added to the wild-type enzyme, the SQ signal was abolished.

OLIS rapid scanning monochromator as described previously (22). Reactions were started by rapid mixing of 3 μM enzyme (expressed as monomers of the bc_1 complex) in assay buffer containing 50 mM phosphate (pH 7.0), 1 mM sodium azide, 0.2 mM EDTA, 0.05% Tween 20, and, where indicated, 1.2 eq of stigmatellin or myxothiazol/bc_1 complex monomer and varying concentrations of DBQ against an equal volume of the same buffer (without enzyme and inhibitors) containing 48 μM DBH_2. For each experiment, 12–16 data sets were averaged, and the oxidized spectrum was subtracted. The time course of the absorbance change at 562 and 578 nm was extracted using software from OLIS. Using the ORIGIN program, the difference between the two wavelengths was plotted and fitted to a second- or third-order exponential, and the fitted curve was then used as the basis for an iterative smoothing procedure to decrease the noise levels of the kinetic traces. In this procedure, the difference between each data point and the corresponding value of the fitted curve at the same time point was calculated and decreased by half.

Kinetic Modeling—The DynaFit program (BioKin, Ltd.), which allows fitting to reaction mechanisms described as a series of individual reaction steps (28), was used to fit the time-dependent b_H reduction through center N. An extinction coefficient of 36 mM^{-1} cm^{-1} was used for this heme group (12, 29). Association and dissociation of DBH_2, DBQ, QH_2, and Q were included together with the corresponding electron transfer reactions into single steps, thereby reducing the number of intermediate species. SQ species formed from partial reduction or oxidation of DBH_2 or endogenous Q were assumed not to dissociate from the enzyme. Electron equilibration between the two b_H hemes in the dimer through the b_L hemes (12) was described as a single step. For b_H reduction in the myxothiazol-inhibited enzyme, the two models used assumed that all ligands were able to bind and react with both b_H hemes in the dimer with identical rate constants. One of the models considered only one center N to be accessible initially, with the second center N being rapidly activated by SQ formation at the first site. When stigmatellin was present, the model used to fit the reduction kinetics assumed different kinetic parameters in one of the two center N sites in the dimer from the outset. The complete DynaFit script files are available as supplemental material.

RESULTS

EPR Spectra of Semiquinone Bound at Center N—The purified yeast cytochrome bc_1 complex has been reported to exhibit an EPR signal centered at g = 2 attributed to an SQ radical (6). However, that putative SQ signal was significantly different from SQ signals reported in other bc_1 complexes (13–15) in that it had a much smaller intensity (only 5% of the Q content), yielded an E_m for SQ that was ~100 mV higher than in other organisms, and was pH-independent. No evidence was provided to demonstrate that such an EPR signal came from a center N radical. As shown in Fig. 1, we have now obtained an EPR signal (g = 2.004 and line width = 0.9 mT) that clearly corresponds to SQ bound at center N, as judged by its sensitivity to three different center N inhibitors (antimycin, funiculosin, and ilicicolin H) and by its absence in bc_1 complex lacking Q. The maximum intensity of this SQ signal at a microwave power of 0.01 milliwatt varied between 0.06 and 0.27/bc_1 complex monomer, depending on the Q content of the enzyme preparation, and occurred at an E_m of 50–60 mV at pH 7.4, in agreement with what has been observed in other bc_1 complexes (13–15).

It was previously shown experimentally (30, 31) and confirmed theoretically (7) that the SQ bound at center N is anti-ferromagnetically coupled to the oxidized b_H heme. Thus, to determine the true concentration and E_m of SQ bound at center N, a correction needs to be made for the portion of the SQ that is EPR-silent due to this coupling. Because the reported E_m of yeast cytochrome *b* using either circular dichroism or EPR spectroscopy was found to be dependent on the type of detergent present (6), we performed a spectrophotometric redox titration of the *b* hemes in the presence of dodecyl maltoside in the same buffer as that used for our EPR experiments.

As shown in Fig. 2*A*, at pH 7.4, the b_H heme has an E_m of ~60 mV. Using this value, we calculated the total percentage (relative to bc_1 monomers) of SQ bound at all center N sites at

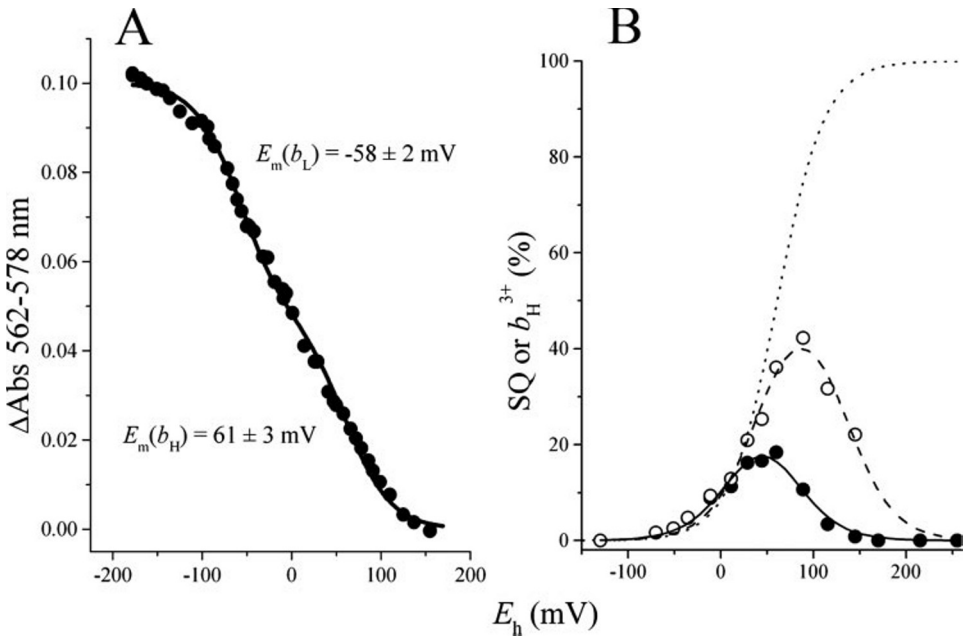

FIGURE 2. **Redox titration of cytochrome *b* and the center N SQ.** Reduction of cytochrome *b* (*A*) as a function of redox potential (E_h) was fitted to Equation 1. The relative b_H contribution to total absorbance (parameter *b* in Equation 1) was 48 ± 1.2%. See supplemental Fig. S1 for a deconvolution of this fit and its comparison with a single Nernst component. The E_m for b_H was used to calculate the total relative concentration of oxidized b_H heme at each E_h value (*dotted line*) in *B*. The intensity of the SQ signal determined by EPR spectroscopy (●) was fitted to Equation 3 (*solid line*), yielding $E_{m(SQ/Q)}$ = 73.1 ± 7.7 mV, $E_{m(QH_2/SQ)}$ = 16.5 ± 7.5 mV, and *C* = 35.1 ± 8.3%. The total SQ bound at center N (○) was calculated using Equation 2. Fitting of the resulting SQ values to Equation 3 (*dashed line*) yielded $E_{m(SQ/Q)}$ = 133.7 ± 6.4 mV, $E_{m(QH_2/SQ)}$ = 39.8 ± 5.1 mV, and *C* = 55.3 ± 5.5%.

different redox potential values ($SQ_{tot}^{E_h}$) from the g = 2.0 EPR signal, which reflects only SQ bound in the vicinity of b_H^{2+} heme complexes ($SQ_{b_H^{2+}}^{E_h}$), expressed as a percentage relative to bc_1 monomers) by applying Equation 2.

$$SQ_{tot}^{E_h}(\%) = \frac{SQ_{b_H^{2+}}^{E_h}(\%)}{1 - \frac{b_H^{3+}(\%)}{100}} \qquad \text{(Eq. 2)}$$

This equation implies that, for instance, when the b_H heme is half-reduced (at E_h = 61 mV), if the EPR-detectable $SQ_{b_H^{2+}}$ amounts to 15%/bc_1 monomer, an additional 15% of the EPR-invisible SQ is expected to be bound to center N sites in which the b_H heme is oxidized. Therefore, SQ can be estimated to occupy 30% of the total center N sites, half of which have b_H^{2+} and the other half b_H^{3+}. At a higher E_h of 120 mV, detecting 3% of SQ/bc_1 monomer by EPR implies that, because only 10% of center N sites have b_H^{2+}, SQ is present in 30% of all center N sites, 90% of which have b_H^{3+}, preventing EPR detection of SQ bound to them. An important assumption made in Equation 2 is that center N binds SQ with equal affinity irrespective of the redox state of the b_H hemes, which is supported by redox titrations in the bovine bc_1 complex that suggest a constant E_m of the b_H heme in the presence or absence of SQ (7). As shown in Fig. 2*B*, the total SQ obtained using Equation 2 yielded a maximum of 40% total SQ/bc_1 monomer at ~90 mV. Because the EPR-observable SQ was zero beyond ~150 mV, the total SQ could not be calculated at higher E_h values, as is evident from Equation 2.

The Nernst equation shows that it is thermodynamically impossible to have a redox couple in which the oxidized or reduced species reaches a concentration of exactly 100%. Therefore, the denominator in Equation 2 will never reach a value of exactly zero, which would result in a mathematical indeterminacy. Also, because by definition $SQ_{b_H^{2+}}^{E_h}$ cannot be larger than the percentage of center N sites that have b_H^{2+}, the $SQ_{tot}^{E_h}$ value will always be <100% of the total center N sites, even at high E_h values. For example, even at an E_h at which the b_H heme is 99% oxidized, $SQ_{b_H^{2+}}$ will be ≤1% simply because only 1% of all the center N sites have a reduced b_H heme that allows EPR detection of a bound SQ. Therefore, applying Equation 2 in this case would yield values of 1 or less in the numerator and 0.01 in the denominator, resulting in an $SQ_{tot}^{E_h}$ value of ≤100%.

The E_m values of the QH_2/SQ and SQ/Q couples were calculated by fitting the experimental data points ($SQ_{b_H^{2+}}^{E_h}$) as well as the predicted $SQ_{tot}^{E_h}$ concentrations to the following Nernst equation (Equation 3),

$$SQ^{E_h}(\%) = (C)\left(\frac{e^{\frac{nF}{RT}(E_{m(SQ/Q)} - E_h)}}{1 + e^{\frac{nF}{RT}(E_{m(SQ/Q)} - E_h)}} - \frac{e^{\frac{nF}{RT}(E_{m(QH_2/SQ)} - E_h)}}{1 + e^{\frac{nF}{RT}(E_{m(QH_2/SQ)} - E_h)}}\right) \qquad \text{(Eq. 3)}$$

where *C* corresponds to the theoretical concentration of SQ/monomer (as a percentage) that could be achieved if the $E_{m(SQ/Q)}$ and $E_{m(QH_2/SQ)}$ values were separated enough to allow maximum accumulation. Its value was ~35% for the EPR-detectable SQ and ~55% for the total SQ calculated from Equation 2. The fitted E_h at which maximum SQ occurred, which is the mean of the two individual E_m values with their respective deviation, yielded values of 44.8 ± 7.6 mV for $SQ_{b_H^{2+}}$ and 86.8 ± 5.3 mV for SQ_{tot}. Therefore, the peak in total bound SQ occurred when the b_H heme was 75% oxidized, implying that, at pH 7.4, SQ stabilization favors the formation of SQ·b_H^{3+} complexes compared with SQ·b_H^{2+} by a factor of 3. Considering that the Q pool in membranes has an E_{m7} reported to be between 60 (6) and 90 (9, 19) mV and that this value changes by −60 mV/pH unit, SQ bound at center N showed an E_m 24–54 mV higher than unbound Q at pH 7.4. This implies that QH_2 binds to center N between 2.5- and 8.3-fold tighter than Q.

Reduction Kinetics of Heme b_H through Center N in the Presence of DBQ—When DBH_2 is added to center P-inhibited bc_1 complex, electrons equilibrate with the b_H hemes only by entry through center N (12). As shown in Fig. 3, addition of increasing

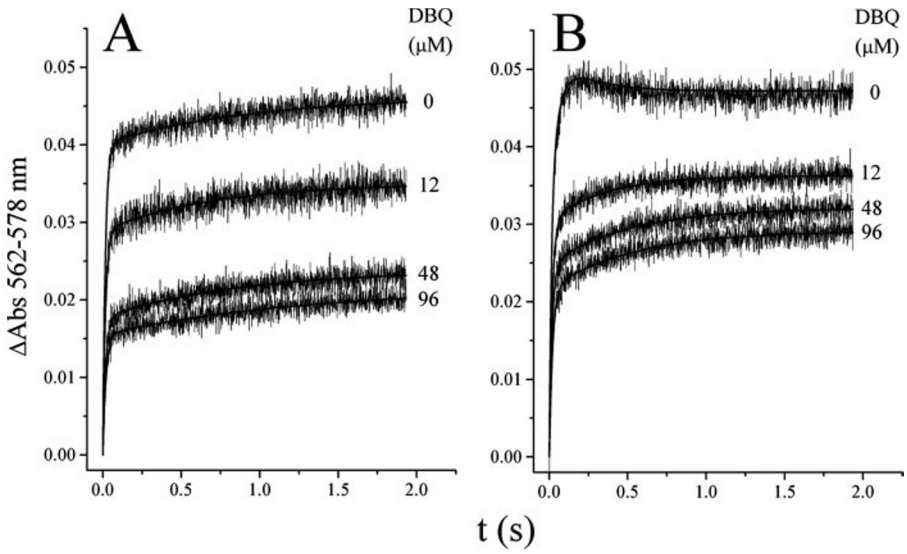

FIGURE 3. **Cytochrome *b* reduction kinetics through center N in the presence of DBQ.** The purified yeast bc_1 complex (1.5 μM) was preincubated with 1.2 eq of myxothiazol (*A*) or stigmatellin (*B*) per monomer and the indicated concentrations of DBQ before rapid mixing with 24 μM DBH_2. For clarity, the traces with 6 and 24 μM DBQ are not shown. All traces were fitted to a double exponential equation, except for the *upper trace* in *B* (without added DBQ), which was fitted to a triple exponential equation. An absorbance difference of 0.052 corresponds to one b_H heme reduced per bc_1 dimer.

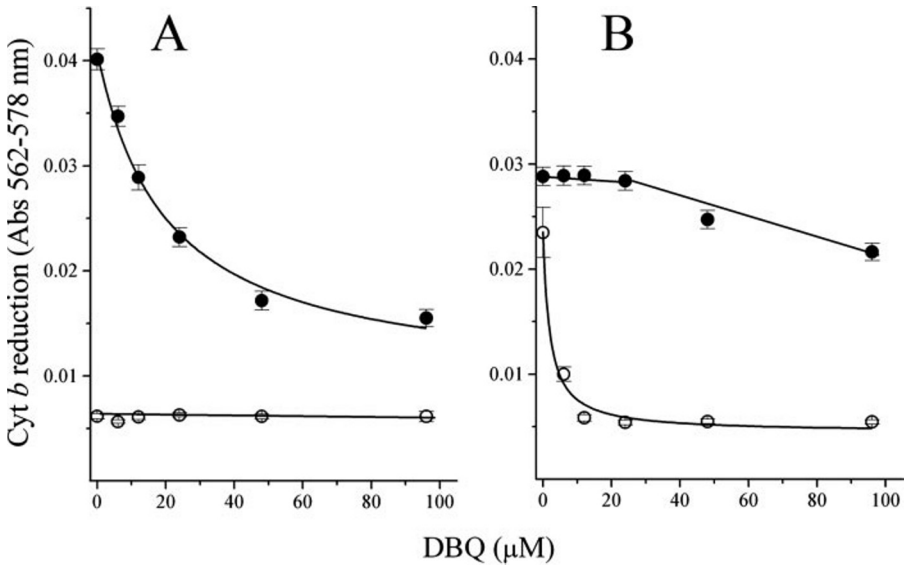

FIGURE 4. **Effect of DBQ on the extent of cytochrome *b* reduction.** The amplitude of the fast (●) and slow (○) reduction phases observed after fitting the data from Fig. 3 in the presence of myxothiazol (*A*) or stigmatellin (*B*) is shown at each DBQ concentration. The fast phase in *A* was fitted to a partial inhibition equation that yielded an affinity of 12 μM for DBQ and a limit of 0.01 *A* for b_H heme oxidation. The slow phase in *B* was fitted to the same equation, with values of 1.4 μM for DBQ affinity and 0.005 *A* for the limit of b_H oxidation. *Cyt*, cytochrome.

concentrations of DBQ resulted in a progressively smaller decrease in the extent of b_H reduction. Interestingly, this oxidation of cytochrome *b* by DBQ was only partial, reaching a limit of ~40% (with myxothiazol) or ~60% (with stigmatellin) of the total extent observed without added DBQ. As reported previously (32), b_H reduction by DBH_2 through center N showed biphasic kinetics when center P was inhibited with myxothiazol (Fig. 3*A*), whereas the presence of stigmatellin resulted in an additional re-oxidation phase that was abolished when DBQ was added (Fig. 3*B*).

Myxothiazol and stigmatellin affected differently the way in which DBQ decreased the extent of the two kinetic components of b_H reduction (Fig. 4). Only the fast phase of b_H reduction was decreased in its magnitude in the presence of myxothiazol (Fig. 4*A*), with an estimated K_m for DBQ oxidation of 12 μM. This contrasted with what was observed with stigmatellin, where the extent of reduction during the slower phase was greatly decreased by low concentrations of DBQ (K_m = 1.4 μM), and the fast reduction showed a modest decrease in its extent only above 30 μM DBQ (Fig. 4*B*). The slower reduction phase in the presence of stigmatellin contributed much more to the total extent of reduction (45%) than that in the presence of myxothiazol (13%), although this contribution became less as DBQ was added.

The rate of the fast phase of b_H reduction was insensitive to DBQ concentration, irrespective of the center P inhibitor present (Fig. 5). This is a surprising result, considering that the b_H oxidation effect of DBQ shown in Fig. 3 demonstrates that DBQ can bind efficiently to center N. If DBQ is assumed to bind to center N in the oxidized bc_1 complex with the same affinity as that calculated from the oxidation of the b_H heme, a significant decrease in the rate of reduction by DBH_2 should have been expected (as simulated by the *dashed lines* in Fig. 5). This result indicates that DBQ does not compete with DBH_2 for binding to center N when the b_H heme is oxidized. DBQ decreased the rate of the slower phase of b_H reduction in the presence of stigmatellin to a value similar to that observed with myxothiazol, which was unaffected by DBQ. A K_m of 2.7 μM was calculated for DBQ based on this decrease in the slow rate.

EPR Spectra of the Center N Semiquinone in the Presence of Center P Inhibitors—To determine the cause of the different b_H reduction kinetics observed in the presence of myxothiazol and stigmatellin, we examined the properties of the EPR-detectable SQ in the absence and presence of these inhibitors (Fig. 6). The intensities and E_m values of SQ in the uninhibited and myxothiazol- and stigmatellin-bound bc_1 complexes were very similar, within experimental error (Fig. 6*A*), indicating that the center P ligand had no effect on the stability of SQ at center N. The power saturation behavior of the SQ signal was also the same under the three conditions (Fig. 6*B*), implying that the relaxation

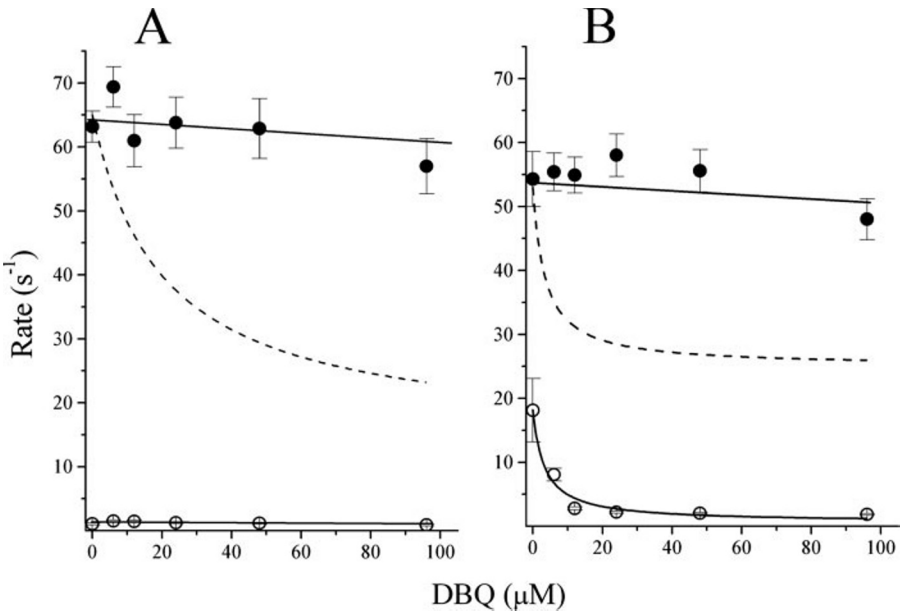

FIGURE 5. **Effect of DBQ on the rate of cytochrome *b* reduction.** The fitted rate values of the first (●) and second (○) reduction phases from the data in Fig. 3 with myxothiazol (*A*) or stigmatellin (*B*) are plotted as a function of DBQ concentration. The slower reduction phase in *B* was the only one to show a significant change as DBQ was increased and was fitted to a simple inhibition equation that generated a K_m of 2.7 μM for oxidation by DBQ. *Dashed lines* show the expected decrease in the rate of reduction by DBH_2 that should have been observed if DBQ was able to bind to the oxidized bc_1 complex with affinities similar to those obtained in Fig. 4 for binding to center N with reduced b_H heme.

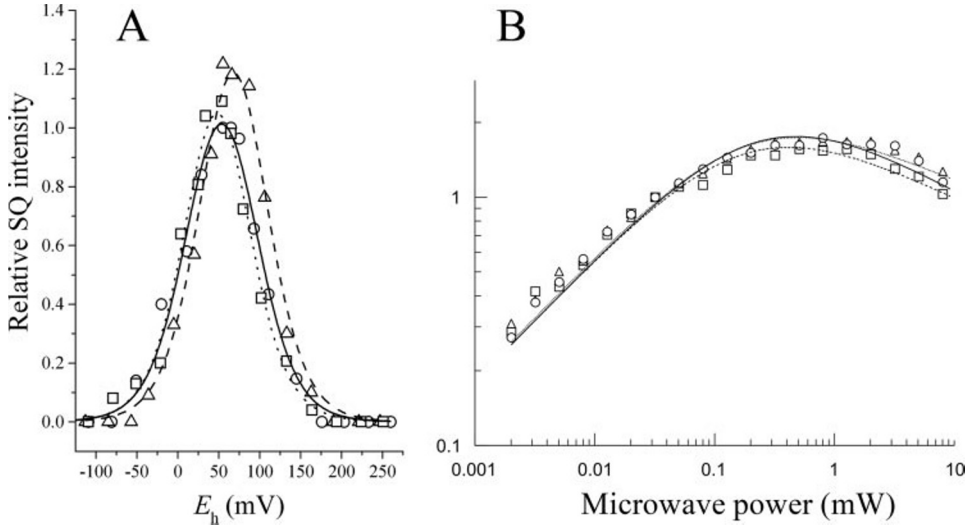

FIGURE 6. **EPR properties of center N SQ in the presence or absence of center P inhibitors.** *A* shows EPR spectra recorded at different E_h values using 27 μM bc_1 complex without inhibitors (○) or in the presence of equimolar concentrations of myxothiazol (□) or stigmatellin (△). SQ signal intensity was normalized to the maximum obtained in the uninhibited enzyme. Redox titrations in *A* were fitted to the same Nernst equation as in Fig. 2. *Solid line*, control; *dashed line*, stigmatellin; *dotted line*, myxothiazol. For the three conditions, fitted E_m values using Equation 3 were within 10 mV of $E_{m(QH_2/SQ)}$ = 30 mV and $E_{m(SQ/Q)}$ = 80 mV. *B* shows the power saturation behavior of the three EPR samples each poised at ~55 mV taken from redox titrations presented in *A*. The half-saturation parameter and maximum SQ concentration varied around 0.21 ± 0.04 milliwatts and 2.4 ± 0.1 μM, respectively, for the three conditions.

properties that report the electronic environment of the unpaired electron in SQ are also independent of the center P inhibitors. These results suggest that changes in center N that are responsible for differences in b_H reduction kinetics when stigmatellin is present are probably short-lived, as we have suggested in previous work (32), and disappear during the several minutes needed to equilibrate the enzyme to the applied E_h in the EPR experiments.

Kinetic Modeling of Center N Kinetics—The observations that DBQ had no effect on the initial rate of b_H reduction and decreased only partially its extent were included in a kinetic model in which DBH_2 and DBQ bind only to center N when b_H is oxidized and reduced, respectively. The kinetic model also included an intermonomeric electron equilibration between b_H hemes in the dimer (see supplemental material for fitted parameters and details on the models). When fitting the kinetic traces obtained in the presence of myxothiazol (Fig. 7*A*), such a model was able to reproduce the partial decrease in the extent of b_H reduction as well as the constant initial rate of reduction by DBH_2 as DBQ was varied. It was impossible to model this behavior in a model in which electron equilibration between monomers does not exist (data not shown), just as we have shown in previous work (12), in which the pre-steady-state kinetics of cytochrome *b* reduction at different QH_2 and antimycin concentrations could be modeled only assuming b_L-to-b_L electron transfer within the dimer. In that same work (12), we showed that this intermonomeric electron equilibration between center N sites occurs despite the thermodynamically unfavorable electron transfer from b_H to b_L.

A small but fast re-oxidation phase that was not found in the experimental data was generated by the model shown in Fig. 7*A*. This was a consequence of allowing DBH_2 binding simultaneously to both center N sites in the oxidized dimer, which resulted in favoring the formation of two $SQ{\cdot}b_H^{2+}$ complexes during the initial moments of the reaction. In this scenario, DBQ (or endogenous Q) could bind only after QH_2 reformed by re-oxidation of one b_H heme by equilibration with SQ and then abandoned center N. An electron would then be transferred from the remaining $SQ{\cdot}b_H^{2+}$ complex in the dimer by intermonomeric electron transfer to yield a reduced b_H heme with an empty center N to which DBQ or Q could bind.

A marked improvement in the fitting was obtained if the model was modified to include the condition that initial

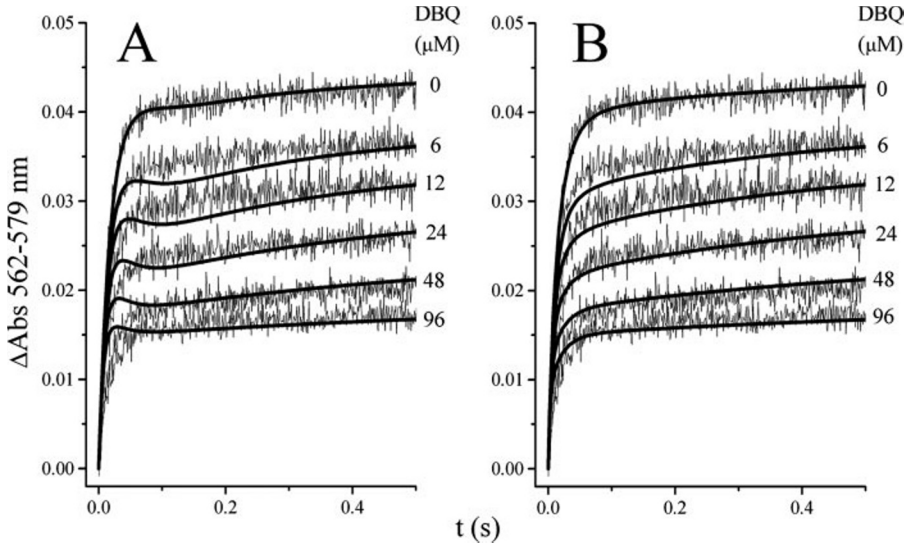

FIGURE 7. **Kinetic modeling of the effect of DBQ on center N kinetics in the presence of myxothiazol.** The kinetic traces obtained as described for Fig. 3*A* were fitted to two DynaFit models (see supplemental material for details). Both models assumed exclusive binding of QH_2 when the b_H heme was oxidized and of Q when the heme was reduced. The model in *A* allowed simultaneous binding of ligands to both center N sites in the dimer, whereas the model in *B* allowed initial binding to only one center N, after which SQ formation transmitted a conformational change to allow binding and reaction at the other monomer. *Solid curves* represent the best fit to each model. Only the first 500 ms of cytochrome *b* reduction are shown to evidence more clearly the difference between the kinetic traces and the fitted curves.

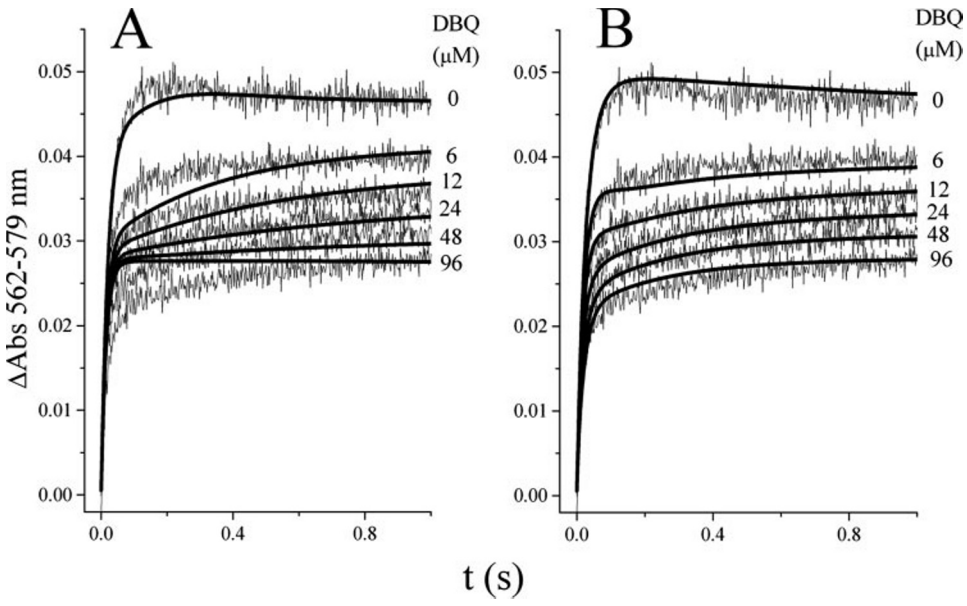

FIGURE 8. **Kinetic modeling of the effect of DBQ on center N kinetics in the presence of stigmatellin.** The kinetic traces obtained as described for Fig. 3*B* were fitted to two DynaFit models. The first model (*A*) assumed equal kinetic properties for both center N sites in the dimer. The second model (*B*) assumed different kinetic properties in each center N site of the dimer in addition to a slow conformational change ($k = 0.15\ s^{-1}$) that resulted in both monomers acquiring the same kinetic properties (see supplemental material for details). Both models assumed exclusive binding of QH_2 when the b_H heme was oxidized and of Q when the heme was reduced. *Solid curves* represent the best fits to each model. Only the first 900 ms of cytochrome *b* reduction are shown to evidence more clearly the difference between the kinetic traces and the fitted curves.

binding of DBH_2 to the oxidized bc_1 complex occurred to only one center N in the dimer (Fig. 7*B*). In this mechanism, SQ formation in this initially active monomer would activate the other center N, allowing DBQ/Q to bind before DBH_2 once the b_H heme in this second monomer receives an electron by intermonomeric electron transfer from the first b_H heme. In this way, formation of two $SQ{\cdot}b_H^{2+}$ complexes in the dimer is avoided as long as DBQ or Q is present, obviating the need for b_H re-oxidation. The fitted values for the rates of intermonomeric electron transfer and activation of the second center N after the initial SQ formation in one monomer were higher than all other rates, suggesting that these two processes were not rate-limiting.

Because endogenous QH_2 was not initially present and was expected to be formed in very small amounts by reduction of SQ in $SQ{\cdot}b_H^{2+}$ complexes, its rate of binding and reduction of the b_H heme could not be accurately determined by the fitting, resulting in very low values with large deviations, especially in the model shown in Fig. 7*A*. Except for this value and the nonlimiting rate of center N activation after the first SQ formation (Fig. 7*B*), all other rate values showed little deviations (see supplemental material), indicating the relevant role of each kinetic step in determining the accuracy of the fit.

Center N kinetics in the presence of stigmatellin as the center P inhibitor were considerably more complicated than those with myxothiazol. Still, we were able to fit the DBQ-independent rate of initial DBH_2 reduction together with the partial decrease in the extent of b_H reduction by assuming that DBH_2 binds to center N only when the b_H heme is oxidized and DBQ/Q only when the b_H heme is reduced (Fig. 8). However, when both center N sites in the dimer were assumed to have the same kinetic properties, the effect of increasing DBQ concentrations on the slow phase of b_H reduction was not accurately fitted (Fig. 8*A*). This model was the same as that used for fitting the center N kinetics in the presence of myxothiazol as shown in Fig. 7*A*. If the model was modified to include the condition that initial binding of DBH_2 to the oxidized bc_1 complex occurred to only one center N in the dimer followed by a fast activation of the second monomer upon SQ formation, which improved the fitting in the presence of myxothiazol as shown in Fig. 7*B*, the data in the presence of stigmatellin showed an even worse fit (data not shown).

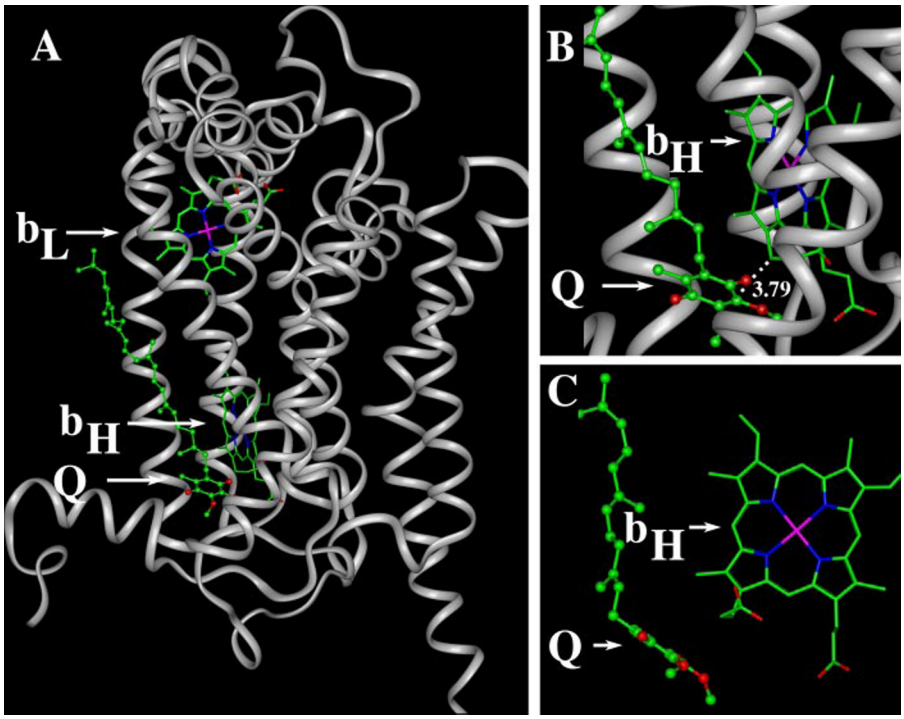

FIGURE 9. **Relationship of the ubiquinone ring to the b_H heme at center N.** The figure was constructed from the coordinates of the crystal structure of the yeast cytochrome bc_1 complex (Protein Data Bank code 1EZV) showing ubiquinone bound at center N (3). Cytochrome *b* of one bc_1 monomer is shown as a *gray ribbon* in *A*, which also shows ubiquinone as a ball-and-stick figure and the b_H and b_L hemes as stick figures. *Arrows* point to the Q ring of ubiquinone and the b_L and b_H heme groups. Carbon atoms are colored *green*, oxygen atoms are *red*, nitrogen atoms are *blue*, and the heme irons are *pink*. *B* is a close-up view of the center N pocket, showing the proximity of the ubiquinone ring to the b_H heme. The 3.79-Å distance between the two ring systems is indicated by a *dashed line*. *C* shows only ubiquinone and the b_H heme, which have been rotated relative to their orientation in *A* and *B* to illustrate the orthogonal relationship between the tetrapyrrole ring of the heme and the Q ring of ubiquinone.

On the other hand, when the model considered that one center N site exhibited different rates of SQ formation and consumption with respect to the other and also included a slow conformational change ($k = 0.15\ s^{-1}$) that gradually made the second center N display the same kinetic properties as the first one (32), a much more accurate fit was obtained (Fig. 8*B*). This model yielded ratios of SQ-forming/SQ-consuming rates that were 1–3 orders of magnitude higher in one monomer than in the other (see supplemental material for all fitted values). These results imply that the asymmetry in SQ stabilization between monomers is preserved for at least several seconds when stigmatellin is occupying center P, in contrast with what we observed in the presence of myxothiazol, where the conformation allowing asymmetric formation of SQ in the dimer appears to be much more short-lived.

DISCUSSION

Previous attempts to characterize the properties of SQ bound at center N of the cytochrome bc_1 complex concur in two main points (13–15). First, the EPR signal originating from SQ is optimally detectable at pH values of at least 8, at which the E_m of the Q pool falls significantly below that of the b_H heme. Second, the E_m of this EPR-visible SQ is higher than that of the Q pool by 20–60 mV. The only exception to this behavior seems to be the SQ signal observed in the purified yeast bc_1 complex (6), which appeared to be smaller in magnitude and with an E_m higher than that of the b_H heme even at high pH values, casting doubt on the identity of its source. In this work, we have demonstrated that the g = 2.004 signal observed by EPR in the yeast complex is similar to that in other sources in that its E_m is lower than that of the b_H heme and that it genuinely reflects SQ bound at center N as judged by its dependence on Q; its sensitivity to a variety of center N inhibitors (antimycin, funiculosin, and ilicicolin H); and its insensitivity to stigmatellin and myxothiazol, which bind to center P (Figs. 1, 2, and 6). Although the sensitivity of the center N SQ to antimycin was shown previously with the bovine bc_1 complex (13), this is the first demonstration that funiculosin and ilicicolin H eliminate the SQ signal in any species.

The reason the previous study in yeast (6) found such anomalous properties of the SQ signal is probably due to the presence of high concentrations (0.1%) of detergent combinations of Triton and deoxycholate or taurocholate, which are not optimal for bc_1 complex purification and activity and which also induced significant variation in the redox properties of the *b* hemes. Because our SQ determinations were performed using dodecyl maltoside, which yields high activities in bc_1 complexes from a variety of sources (21), the values we have obtained are well in agreement with the rest of the literature.

The observation concerning the increase in the SQ EPR signal mainly at high pH values can be understood by considering that only SQ bound in the vicinity of a reduced b_H heme has paramagnetic properties. The anti-ferromagnetic coupling between the b_H^{3+} heme and SQ bound at center N has already been experimentally demonstrated in the yeast bc_1 complex (30, 31). In those experiments, a strong mismatch between the reduction of the b_H heme as measured by visible spectroscopy and the disappearance of the g = 3.60 EPR signal generated by b_H^{3+} was observed (30), indicating that a paramagnetic species formed in the vicinity of the heme during the early phase of the reductive titration was eliminating the b_H^{3+} EPR signal. Depleting the bc_1 complex of Q eliminated the mismatch between the b_H reduction levels determined by visible and EPR spectroscopy (31), confirming that SQ was the species forming a diamagnetic, exchange-coupled complex with b_H^{3+} that eliminated the EPR signals from both the heme and the Q radical.

As shown in Fig. 9, the crystal structure of the yeast bc_1 complex with Q bound at center N (3) reveals an orthogonal orientation and short distance (<4 Å) between the Q and heme ring

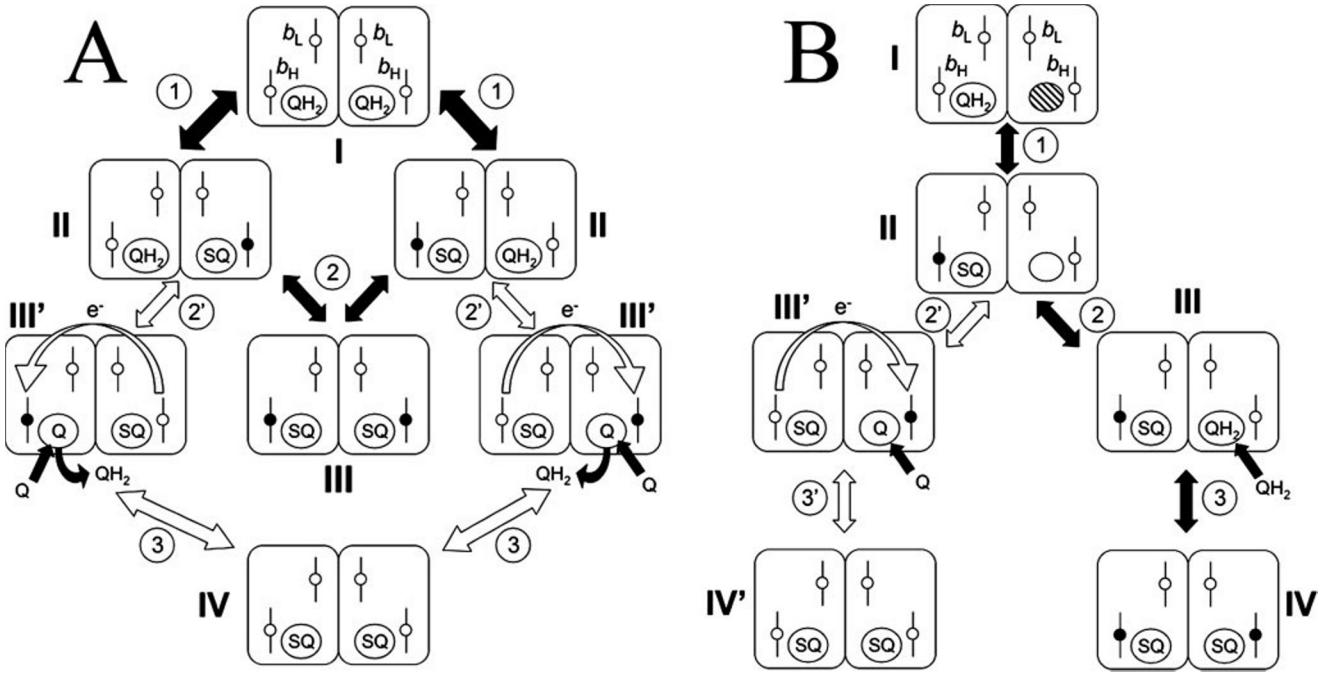

FIGURE 10. **Two models of electron equilibration at center N in the dimeric bc_1 complex.** The model in *A* assumes that QH_2 can bind to any of the two monomers in the oxidized dimer. In the model in *B*, one center N is initially inactive (indicated by the *hatched circle*). Cytochrome *b* dimers are shown as *paired rectangles*, with center N sites as *circles* next to the b_H hemes. All other subunits, as well as center P reactions, have been omitted for clarity. Different dimer intermediates in the reaction sequence are labeled with *roman numerals* and joined to each other by reversible steps represented by *double-headed arrows*. *White arrows* are steps that depend on electron (e^-) transfer events from one b_H heme to the other via the b_L hemes. The oxidation state of the b_H heme is shown: reduced (●) or oxidized (○). The two models are compared under "Discussion."

systems that apparently allow an interaction between the magnetic fields of the unpaired electrons from both species. Interestingly, a very similar orientation and distance are present between the b_H heme and a *c*-type heme in the homologous b_6f complex that occupies a position equivalent to that of Q in the bc_1 complex (33). Recent work has demonstrated a strong coupling between the electrons of these two hemes as revealed by their EPR spectra (34). This provides further evidence that the relative positions of the b_H heme and SQ in the bc_1 complex are conducive to the formation of an EPR-invisible complex.

After correcting for the amount of EPR-invisible SQ at center N, it becomes evident that most of the SQ at physiologically relevant pH values exists bound close to the oxidized b_H heme (Fig. 2). This had already been proposed to occur at pH 7.05 in simulations that tried to explain the significant increase in the E_m of a fraction of the b_H heme population (7). It is noteworthy that those simulations assumed that Q bound at center N increases the E_m of the b_H heme by 68 mV (7). Although nothing was discussed in that work with respect to the binding of Q and QH_2 to center N, the thermodynamic consequence of such a shift in the E_m of the b_H heme is that Q should be expected to bind with an affinity ~14 times higher when the b_H heme is reduced than when it is oxidized. We now show that DBQ oxidizes the b_H heme with a K_m of 1.4–12 μM (Figs. 3–5), which gives a relative measure of the affinity of center N for Q when the b_H heme is in the reduced state. In contrast, ~100 μM DBQ was unable to compete against DBH_2 for binding to center N when the enzyme was oxidized. This indicates that, as can be deduced from the effects of Q on the E_m of the b_H heme (7), binding of the oxidized substrate to center N is favored by one to two orders of magnitude when the b_H heme is reduced.

The second common conclusion from EPR studies of SQ at center N, that the E_m of this species is higher than that of the Q pool, has been interpreted as indicative of a tighter binding of QH_2 than Q to this site (13–15). After correcting for the EPR-invisible SQ bound close to b_H^{3+} (Fig. 2), we also conclude that the peak of SQ occurs at an E_m higher than expected for the unbound QH_2/Q couple. We propose that this minimizes formation of $SQ{\cdot}b_H^{2+}$ complexes, which, as we have discussed elsewhere (12), favor superoxide formation at center P due to the absence of electron acceptors in cytochrome *b*. However, a tighter binding of QH_2 at center N would by itself inhibit electron flow out of cytochrome *b* by inhibiting binding of Q. This potential problem can be circumvented by assuming that QH_2 binds poorly to center N when the b_H heme is reduced, but tightly when the heme is oxidized. As discussed above, Q binds with an opposite redox preference, thereby avoiding competition from QH_2. This redox specificity in binding to center N would also ensure that QH_2 leaves center N whenever electrons from center P arrive at the b_H hemes.

We have already provided evidence pointing to a deficient binding of QH_2 to the reduced bc_1 complex by analyzing the kinetics of antimycin binding to center N (32). In that work, we reported that DBH_2 concentrations much higher than those needed for binding to center N when the enzyme is oxidized do not decrease the binding rate of antimycin when the enzyme is reduced with dithionite. It is well known that the few equivalents of Q copurified with the bc_1 complex are sufficient to sustain high turnover rates when steady-state activity is measured (21). Although this endogenous Q complement is diluted together with the enzyme to nM concentrations in such assays, μM concentrations of DBH_2 or other QH_2 analogs do not

appear to out-compete Q at center N. DBQ added to such assays does not activate the enzyme, but rather inhibits it by competing against DBH_2 at center P (35). These observations are consistent with our proposal that Q binds to center N without interference from QH_2 even at extraordinarily high QH_2/Q ratios. Our present results also agree with the assumption of a redox-specific binding of QH_2 and Q to center N that depends on the oxidation state of the b_H heme. The immediate decrease in the extent of cytochrome *b* reduction through center N at concentrations of DBQ much lower than those of DBH_2 indicates a noncompetitive binding pattern between the two Q species, as confirmed by fitting to kinetic mechanisms that incorporate that assumption (Figs. 4–7). In contrast, SQ is expected to bind independently of the b_H redox state. As we have discussed previously (32), this is the case with antimycin, which we consider to be an analog of SQ.

The redox-specific binding of QH_2 and Q to center N might seem to be unsupported by crystal structures in which Q is found at center N, where the b_H heme is supposed to be oxidized. However, the redox state of the enzyme and Q in the crystals is not easy to determine after x-ray bombardment, and the high concentrations (up to the mM range) of both enzyme and Q in the crystals could force Q to bind to center N even when the b_H heme is oxidized. Thus, crystallographic data cannot be used to support or argue against redox-specific binding of ligands at center N as measured in this work.

To prevent QH_2 from interfering with oxidation of the b_H heme by Q, another condition must be met. As illustrated by the model in Fig. 10*A*, if only QH_2 is assumed to bind to the oxidized enzyme at center N (*intermediate I*), reduction of the b_H heme in one monomer (*step 1*) will result in a tightly bound SQ (*intermediate II*), which will prevent Q from binding to any center N with b_H^{2+}. After QH_2 oxidation in the other monomer (*step 2*), only dimers with two SQ·b_H^{2+} complexes can be formed (*intermediate III*). However, if the electron in the b_H heme can equilibrate with the other monomer (*step 2′*), QH_2 bound will be displaced as the b_H heme in its proximity receives an electron (*intermediate III′*). Q will then be able to bind and oxidize b_H^{2+} in that second center N (*step 3*), resulting in a dimer with two SQ·b_H^{3+} complexes (*intermediate IV*), which are optimal as acceptors for electrons coming from center P.

However, even assuming that there is electron crossover within the cytochrome *b* dimer, the kinetic data are not explained completely unless conformational communication between center N sites is included. If QH_2 is allowed to bind simultaneously to both center N sites, Q would be able to bind and oxidize the b_H heme only after three events occur: reduction of one b_H heme in the dimer with formation of SQ, electron transfer to the b_H heme in the other monomer, and dissociation of QH_2 bound next to this formerly oxidized heme (Fig. 10*A*, *steps 1*, *2′*, and *3*). This implies that one electron will necessarily have to reside in the dimer during the interchange of Q for QH_2 (*intermediates II′* and *III′*) before leaving the b_H hemes to form a second SQ (*intermediate IV*). Our modeling of center N kinetics in the presence of myxothiazol suggests that this delay in Q binding and b_H re-oxidation should be observable as a triphasic behavior in the presence of DBQ (see the *fitted curves* in Fig. 7*A*).

We have found that a kinetic model that assumes that one center N is initially inactive more accurately fits the center N kinetics that we have observed in the presence of myxothiazol as the center P inhibitor (Fig. 7*B*). As illustrated in Fig. 10*B*, if QH_2 is allowed to bind only to one monomer (*intermediate I*), SQ formation in the active site (*step 1*, *intermediate II*) activates the second center N site to bind either QH_2 (*step 2*) or Q (*step 2′*), depending on whether the electron is still residing in the original monomer (*intermediate III*) or has moved to the other b_H heme by electron crossover (*intermediate III′*). Because the electron has the same probability of residing in either b_H heme, the likelihood of forming a dimer with two SQ·b_H^{2+} (*intermediate IV*) or two SQ·b_H^{3+} (*intermediate V′*) complexes in equilibrium with their respective single SQ forms (*intermediates III* and *III′*) would depend on the relative amount of QH_2 and Q available. Both models described in Fig. 10 assume that QH_2 and Q binding depends on the redox state of the b_H heme. Consequently, either of them would explain why addition of even the highest concentration of DBQ never results in a complete oxidation of cytochrome *b* (Fig. 3). Nevertheless, we have recently presented evidence for conformational communication between center N sites in the dimer (32), supporting the asymmetric binding model shown in Fig. 10*B*, which also provides a better fit to the experimental data.

The more complicated kinetic behavior at center N that we have found in the presence of stigmatellin (Figs. 3*B* and 8) agrees with our previous suggestion that the conformational communication that breaks the asymmetry between the two center N sites is delayed when both Rieske proteins are close to center P (32). However, this delay is not long enough to allow the observation of any difference in the SQ properties once the enzyme is in equilibrium (Fig. 6). This could also explain why Q is found at both center N sites in the dimer in the bc_1 structure even in the presence of stigmatellin (3). Nevertheless, under some conditions, this asymmetry in binding to center N might be retained at least partially and for longer periods of time, as has been reported for the yeast bc_1 complex co-crystallized with cytochrome *c* in the presence of stigmatellin, where Q occupancy at center N is significantly decreased in one monomer, but not completely abolished (36).

The different center N kinetics we have observed in the presence of stigmatellin support the role of long-range communication between centers P and N, as has become increasingly evident by other reports in the literature (37–39). Our present results indicate that, even in the presence of myxothiazol, which does not affect the position of the Rieske protein (40), intradimer electron transfer, together with the b_H redox-dependent and asymmetric binding of QH_2 and Q, is relevant to ensure proper center N function in the bc_1 complex dimer. All of these effects serve to control SQ formation in a way that maximizes the availability of b_H^{3+} as acceptor for electrons coming from center P while at the same time promoting the binding of Q and the release of QH_2 at center N whenever the b_H heme undergoes reduction.

Acknowledgment—We thank Ulrich Brandt for providing the EPR facilities.

REFERENCES

1. Xia, D., Yu, C. A., Kim, H., Xian, J. Z., Kachurin, A. M., Zhang, L., Yu, L., and Deisenhofer, J. (1997) *Science* **277,** 60–66
2. Zhang, Z. L., Huang, L. S., Shulmeister, V. M., Chi, Y. I., Kim, K. K., Hung, L. W., Crofts, A. R., Berry, E. A., and Kim, S. H. (1998) *Nature* **392,** 677–684
3. Hunte, C., Koepke, J., Lange, C., Rossmanith, T., and Michel, H. (2000) *Structure Folding Des.* **8,** 669–684
4. Berry, E. A., Huang, L. S., Saechao, L. K., Pon, N. G., Valkova-Valchanova, M., and Daldal, F. (2004) *Photosynth. Res.* **81,** 251–275
5. Dutton, P. L., and Jackson, J. B. (1972) *Eur. J. Biochem.* **30,** 495–510
6. T'sai, A. L., and Palmer, G. (1983) *Biochim. Biophys. Acta* **722,** 349–363
7. Rich, P. R., Jeal, A. E., Madgwick, S. A., and Moody, A. J. (1990) *Biochim. Biophys. Acta* **1018,** 29–40
8. Kröger, A., and Klingenberg, M. (1973) *Biochim. Biophys. Acta* **34,** 358–368
9. Takamiya, K. I., and Dutton, P. L. (1979) *Biochim. Biophys. Acta* **546,** 1–16
10. Kramer, D. M., Roberts, A. G., Muller, F., Cape, J., and Bowman, M. K. (2004) *Methods Enzymol.* **382,** 21–45
11. Muller, F. L., Roberts, A. G., Bowman, M. K., and Kramer, D. M. (2003) *Biochemistry* **42,** 6493–6499
12. Covian, R., and Trumpower, B. L. (2005) *J. Biol. Chem.* **280,** 22732–22740
13. Ohnishi, T., and Trumpower, B. L. (1980) *J. Biol. Chem.* **255,** 3278–3284
14. De Vries, S., Berden, J. A., and Slater, E. C. (1980) *FEBS Lett.* **122,** 143–148
15. Robertson, D. E., Prince, R. C., Bowyer, J. R., Matsuura, K., Dutton, P. L., and Ohnishi, T. (1984) *J. Biol. Chem.* **259,** 1758–1763
16. Trumpower, B. L., and Edwards, C. A. (1979) *J. Biol. Chem.* **254,** 8697–8706
17. Gutierrez-Cirlos, E. B., Merbitz-Zahradnik, T., and Trumpower, B. L. (2002) *J. Biol. Chem.* **277,** 1195–1202
18. Von Jagow, G., and Link, T. A. (1986) *Method Enzymol.* **126,** 253–271
19. Rich, P. R. (1984) *Biochim. Biophys. Acta* **768,** 53–79
20. Gutierrez-Cirlos, E. B., Merbitz-Zahradnik, T., and Trumpower, B. L. (2004) *J. Biol. Chem.* **279,** 8708–8714
21. Ljungdahl, P. O., Pennoyer, J. D., Robertson, D. E., and Trumpower, B. L. (1987) *Biochim. Biophys. Acta* **891,** 227–241
22. Snyder, C. H., and Trumpower, B. L. (1998) *Biochim. Biophys. Acta* **1365,** 125–134
23. Yu, C. A., Yu, L., and King, T. E. (1972) *J. Biol. Chem.* **247,** 1012–1019
24. Berden, J. A., and Slater, E. C. (1970) *Biochim. Biophys. Acta* **216,** 237–249
25. Snyder, C. H., and Trumpower, B. L. (1999) *J. Biol. Chem.* **274,** 31209–31216
26. Ohnishi, T. (1998) *Biochim. Biophys. Acta* **1364,** 186–206
27. Dutton, P. L. (1978) *Methods Enzymol.* **54,** 411–435
28. Kuzmic, P. (1996) *Anal. Biochem.* **237,** 260–273
29. Covian, R., Gutierrez-Cirlos, E. B., and Trumpower, B. L. (2004) *J. Biol. Chem.* **279,** 15040–15049
30. Siedow, J. N., Power, S., De la Rosa, F. F., and Palmer, G. (1978) *J. Biol. Chem.* **253,** 2392–2399
31. De la Rosa, F. F., and Palmer, G. (1982) *FEBS Lett.* **163,** 140–143
32. Covian, R., and Trumpower, B. L. (2006) *J. Biol. Chem.* **281,** 30925–30932
33. Kurisu, G., Zhang, H., Smith, J. L., and Cramer, W. A. (2003) *Science* **302,** 1009–1014
34. Zatsman, A. I., Zhang, H., Gunderson, W. A., Cramer, W. A., and Hendrich, M. P. (2006) *J. Am. Chem. Soc.* **128,** 14246–14247
35. Covian, R., and Moreno-Sanchez, R. (2001) *Eur. J. Biochem.* **268,** 5783–5790
36. Lange, C., and Hunte, C. (2002) *Proc. Natl. Acad. Sci. U. S. A.* **99,** 2800–2805
37. Valkova-Valchanova, M., Darrouzet, E., Moomaw, C. R., Slaughter, C. A., and Daldal, F. (2000) *Biochemistry* **39,** 15484–15492
38. Cooley, J. W., Ohnishi, T., and Daldal, F. (2005) *Biochemistry* **44,** 10520–10532
39. Wenz, T., Covian, R., Hellwig, P., Macmillan, F., Meunier, B., Trumpower, B. L., and Hunte, C. (2007) *J. Biol. Chem.* **282,** 3977–3988
40. Esser, L., Quinn, B., Li, Y. F., Zhang, M., Elberry, M., Yu, L., Yu, C. A., and Xia, D. (2004) *J. Mol. Biol.* **341,** 281–302